ACS Catalysis

Article

Establishing Au nanoparticle size effect in the oxidation of cyclohexene using gradually changing Au catalysts

Baira Donoeva, Daniil Ovoshchnikov, and Vladimir B. Golovko

ACS Catal., **Just Accepted Manuscript** • Publication Date (Web): 06 Nov 2013

ACS Catalysis is published by the American Chemical Society. 1155 Sixteenth Street N.W., Washington, DC 20036

Establishing Au nanoparticle size effect in the oxidation of cyclohexene using gradually changing Au catalysts

Baira G. Donoeva,[†§‡] *Daniil S. Ovoshchnikov,*[†‡] *Vladimir B. Golovko*[†§*]

[†] Department of Chemistry, University of Canterbury, 20 Kirkwood Ave, Christchurch 8041, New Zealand

[§] The MacDiarmid Institute for Advanced Materials and Nanotechnology, New Zealand

KEYWORDS Gold nanoparticles, gold clusters, oxidation, catalysis, size effect.

ABSTRACT The effect of gold nanoparticles' size on their catalytic activity in aerobic oxidation of cyclohexene was established using supported gold nanoparticles that gradually change their size during catalytic reaction. Two triphenylphosphine-stabilized clusters, $Au_9(PPh_3)_8(NO_3)_3$ and $Au_{101}(PPh_3)_{21}Cl_5$, were synthesized and deposited on SiO_2. The clusters did not retain their structure during the catalytic reaction – larger particles with mean diameters of ca. 5-10 nm gradually formed. By combining kinetic experiments with the monitoring catalyst transformations using TEM, diffuse-reflectance UV-visible spectroscopy and XPS, we showed that catalytic activity appeared only after Au^0 particles larger than 2 nm had formed, while intact

clusters and phosphine-free sub-2 nm particles were inactive in cyclohexene oxidation under the studied conditions.

INTRODUCTION

Gold was long considered chemically inactive, until Haruta and Hutchings discovered remarkable catalytic properties of gold nanoparticles in their pioneering works.[1,2] Since that discovery, gold nanoparticles were shown to be active in various reactions, including low-temperature CO oxidation, C-C bond formation, selective hydrogenation and oxidation, etc.[3-5] One of the crucial parameters determining the catalytic activity of gold is the size of gold particles, e.g. only particles with sizes below 5 nm are active in the low-temperature CO oxidation and their activity increases with decrease of the particle size.[6-9] Attempts were also made to establish particle size effects for the liquid-phase oxidation reactions catalyzed by supported gold nanoparticles. However, opposite trends in the effects of Au particle size on their catalytic activity in the same reactions are frequently reported.[10-16] Typically, particle size effects are studied by comparing catalytic activities within a series of supported gold nanoparticles with different mean diameters which are assumed to be constant during the reaction.[12,14,17,18] Gold particles within such series are often prepared using different wet chemistry methods, which could affect the catalytic activity thus obscuring the effect of the particle size. Such influence could be eliminated by employing gold particles that gradually change their size during the catalytic reaction. Because catalytic activity can be observed only when active sites are present, simultaneous monitoring of the catalytic activity and the state of catalyst in such gradually changing system could provide insight regarding the optimal catalyst morphology. In this work, we employed silica-supported phosphine-stabilized Au clusters with initial sizes below 2 nm and studied their activity in aerobic oxidation of cyclohexene used as a model reaction. We found

that the clusters were unstable during the reaction and gradually agglomerated to form larger particles. By combining the investigation of cyclohexene oxidation kinetics with the monitoring catalyst transformations we established an Au nanoparticles size effect on their catalytic activity.

RESULTS AND DISCUSSION

Triphenylphosphine-stabilized gold cluster, $Au_9(PPh_3)_8(NO_3)_3$ (Au_9), and gold nanoparticles with an estimated composition of $Au_{101}(PPh_3)_{21}Cl_5$ (Au_{101}), with mean gold core diameters of 0.9 and 1.5 nm, respectively, were immobilized on SiO_2. The catalysts were denoted by xAu_n/SiO_2, where x indicates Au loading (wt%). The catalysts were tested in the aerobic solvent-free oxidation of cyclohexene at 65 ˚C. Four major products formed during the reaction: cyclohexene oxide, 2-cyclohexene-1-ol, 2-cyclohexene-1-one and cyclohexenyl hydroperoxide with the latter being the main product. We observed an induction period in the oxidation of cyclohexene, catalyzed by as made Au_n/SiO_2. The length of the induction period depended on the Au loading of the catalyst (Figure 1A). The decrease of the Au loading of Au_9/SiO_2 from 0.5 to 0.02 wt% led to the elongation of the induction period from ca. 1 to 6.5 h. The length of the induction period also depended on the type of Au cluster: $0.1Au_{101}/SiO_2$ showed a significantly shorter induction period of 50 minutes compared with 3.5 hours for $0.1Au_9/SiO_2$ (Figure 1B).

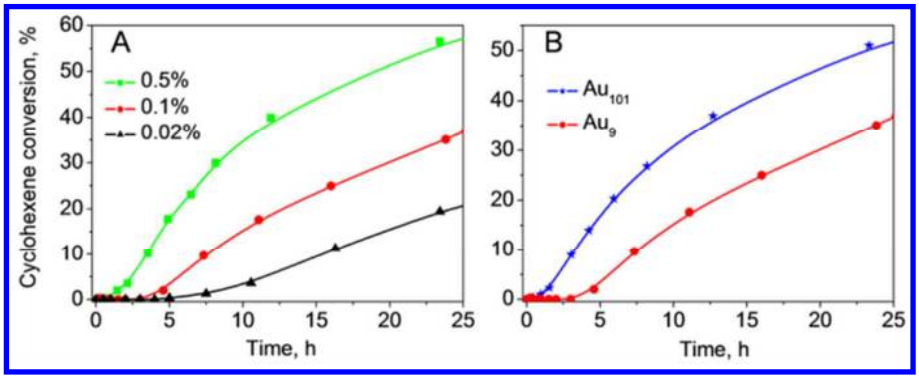

Figure 1. Cyclohexene oxidation catalyzed by A) Au_9/SiO_2 with gold loadings of 0.5, 0.1 and 0.02% and B) $0.1Au_{101}/SiO_2$ and $0.1Au_9/SiO_2$. Conditions: solvent-free cyclohexene, 10 mL, O_2 1 atm, 65 °C, catalyst 0.1 g.

Change of the Au particle size during the reaction was monitored using TEM and diffuse-reflectance UV-visible spectroscopy (DR UV-vis). TEM micrographs of $0.5Au_9/SiO_2$ sampled from the reaction after 0.5, 1 and 16 h are shown in Figures 2B-D. Intact Au_9 clusters of as made $0.5Au_9/SiO_2$ are not visible on bright-field TEM images because of the poor contrast for the supported Au clusters smaller than 1 nm (Figure 2A). During the reaction larger particles, detectable by TEM, gradually form and their number increases, as evidenced by the increase of the surface density of visible particles: ca. 40, 170 and 370 particles/μm^2 were detected in TEM micrographs of $0.5Au_9/SiO_2$ sampled from the reaction after 0.5, 1 and 16 h, respectively. The mean diameter of detectable particles was 3.1 ± 1.2 nm after 1 h of reaction and it increased further to 5.4 ± 1.4 nm during the next 15 h. The development of the particle size as a function of reaction time for $0.5Au_9/SiO_2$ is shown in Figure S7.

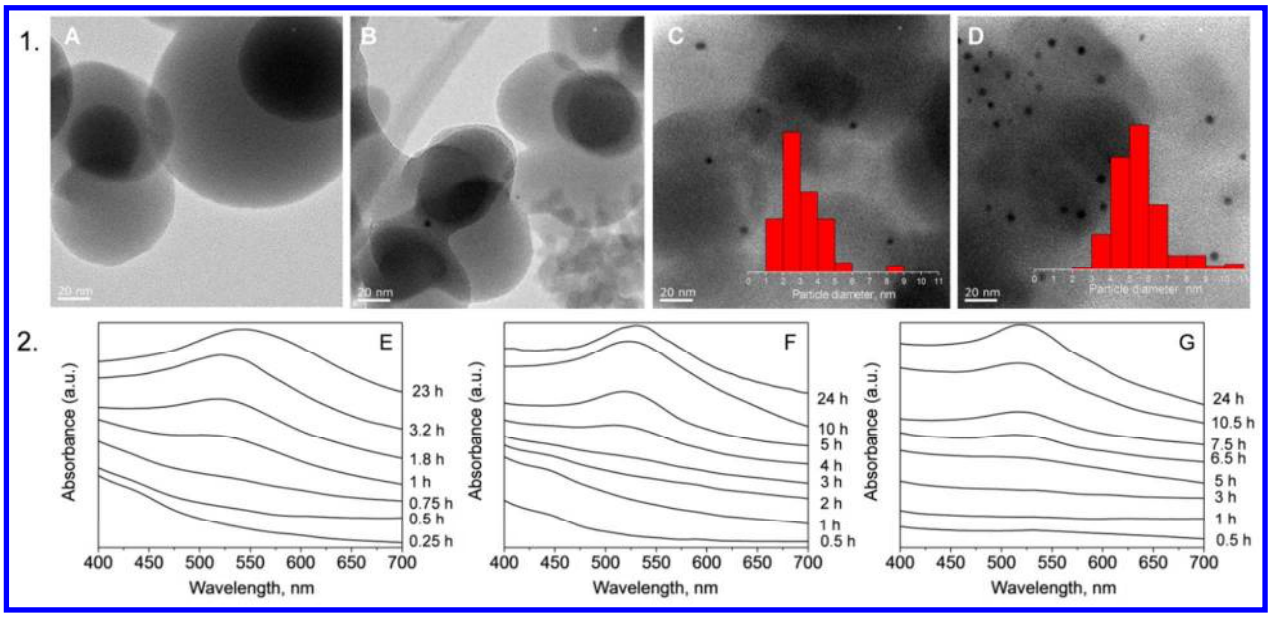

Figure 2. 1) TEM micrographs of $0.5Au_9/SiO_2$ as made (A) and sampled from the reaction after 0.5 h (B), 1 h (C) and 16 h (D); 2) DR UV-vis spectra of $0.5Au_9/SiO_2$ (E), $0.1Au_9/SiO_2$ (F) and $0.02Au_9/SiO_2$ (G) sampled at reaction times indicated along the right-hand ordinates.

DR UV-vis study of $0.5Au_9/SiO_2$ showed the appearance of the surface plasmon resonance (SPR) band at 520 nm for samples of catalyst recovered after 1 h of reaction. The appearance of SPR band indicates the formation of gold particles larger than 2 nm (Figure 2E).[19-21] Hence, both TEM and DR UV-vis studies of $0.5Au_9/SiO_2$ show the similar time of formation of particles larger than 2 nm. DR UV-vis studies of $0.1Au_9/SiO_2$ and $0.02Au_9/SiO_2$ showed that particles larger than 2 nm form only after ca. 4 and 6.5 h, respectively. Slower gold agglomeration for catalysts with lower Au loadings is most likely due to the lower density of Au particles on SiO_2 surface. As seen from the kinetics of cyclohexene oxidation (Figure 1A) and DR UV-vis data, in all cases formation of sufficient number of particles larger than 2 nm was accompanied with the appearance of catalytic activity, which indicates that such particles are active in cyclohexene oxidation. The absence of an induction period for Au_9/SiO_2, recycled after 16 h catalytic run, supports this conclusion (Figure 3).

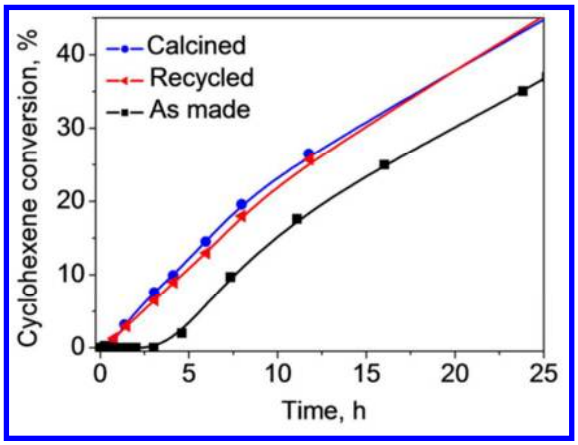

Figure 3. Cyclohexene oxidation catalyzed by as made, recycled and pre-calcined $0.1Au_9/SiO_2$.

Importantly, the cyclohexene used for catalytic oxidation did not contain 2,6-di-tert-butyl-4-methylphenol, which is typically added as a stabilizer by chemical suppliers. When we used cyclohexene which contained the stabilizer, the Au_9 clusters did not agglomerate after 16 hours under typical reaction conditions (65 °C, 1 atm O_2) and no cyclohexene conversion was observed. Stirring $0.5Au_9/SiO_2$ for 16 hours under typical reaction conditions, but in n-hexane instead of cyclohexene, also did not lead to cluster agglomeration. These results imply that thermal treatment at 65 °C alone is not enough to induce agglomeration of Au_9 supported on SiO_2. Recently, Kilmartin et al. reported the removal of phosphine ligands from silica supported $Au_6(Ph_2P(o\text{-tolyl}))_6(NO_3)_2$ by tert-butyl hydroperoxide.[22] We suggest that in our case phosphine ligands were removed from the cluster via reaction with cyclohexenyl hydroperoxide (CyOOH), which is present in trace amounts in the stabilizer-free cyclohexene (ca. 0.015 wt% by GC). Agglomeration did not occur in n-hexane or stabilized cyclohexene because neither of them contained even traces of peroxides. Thus, cluster agglomeration is possible only when PPh_3 ligands are removed from the gold core of Au_9. An indication of such step-by-step in situ transformation of gold clusters, which includes ligand removal from the cluster cores and subsequent particle agglomeration, can also be seen in Figure 2F. DR-UV-vis spectra of catalyst sampled in the initial stages of the reaction possessed a weak band at 450 nm, originating from intact Au_9 clusters (Figure S1C). The features in the optical spectra of small phosphine-stabilized gold clusters are known to be due to the effects of the ligand shell bound to the gold core of the cluster.[23] Therefore, the disappearance of the band at 450 nm before the SPR band emerges indicates that agglomeration occurs after the ligand shell is at least partially removed. Because sintering is not possible when ligands are still bound to the gold cores of the clusters, we conclude that particles forming during the reaction are predominantly phosphine-free.

Pure Au_9 clusters lose phosphine ligands upon calcination at 230°C for 40 min in Ar flow according to TGA (Figure S3). Calcination of $0.1Au_9/SiO_2$ under the same conditions in order to remove phosphine ligands from supported Au_9 led to the formation of 8.0 ± 2.6 nm particles (Figure S10). Catalyst treated this way showed a cyclohexene conversion profile similar to that of the recycled $0.1Au_9/SiO_2$ (particle size 9.6 ± 3.9 nm, SI), which indicates that phosphine-free particles of similar size and larger than 2 nm obtained in different ways have similar activity in the reaction (Figure 3).

Inasmuch as two catalyst parameters change during the reaction, i.e. Au particle size and the presence of phosphine ligands, the initial inactivity of the as made catalysts could be due to one of the following: a) stabilizing ligands cover active gold sites, thus hindering the catalytic activity; once the phosphine ligands are removed, the particles become active b) sub-2 nm gold particles, even without phosphine ligands, are inactive in cyclohexene oxidation and activity appears only after the particle size reaches a certain threshold. Results of our experiments indicate that removal of phosphine ligands is not a sufficient condition for the appearance of catalytic activity and particle size plays a significant role:

a) As seen from Figure 2F, the PPh_3 ligand shell was at least partially removed from Au_9 after 2 hours, as indicated by disappearance of the band at 450 nm, but no activity was observed until particles larger than 2 nm had formed after ca. 4 hours of reaction (Figure 1A).

b) Because the core of Au_{101} is larger than that of Au_9, gold particles derived from Au_{101} need significantly less time to overcome the threshold in particle size, which leads to shorter induction period for Au_{101} catalyst (Figure 1B).

To confirm that small (sub-2 nm) and phosphine-free Au particles are inactive in cyclohexene oxidation, we deposited Au_9 on SBA-15,[24] a mesoporous SiO_2-based material with

large surface area (see SI for details). We used a mixture of ethanol and dichloromethane to ensure homogeneous distribution of clusters throughout the surface of the support.[25] To remove phosphine ligands from the cluster core, the catalyst was calcined at 230 °C for 40 min in Ar flow (denoted as $0.1Au_9$/SBA_c230). The large surface area of the support and the homogeneous distribution of clusters prevented particles from sintering during calcination, as evidenced by the absence of the SPR band in the DR UV-vis spectrum of $0.1Au_9$/SBA_c230 (Figure 4). On the other hand, the absence of absorption bands at 450, 380 and 315 nm, characteristic for the Au_9 cluster, indicates successful removal of ligands during calcination. TEM of $0.1Au_9$/SBA_c230 also confirmed very minimal agglomeration – only a few particles of 2-3 nm were detected, which correlates with the results obtained for Au_{11} clusters in the similar system.[25] Thus, phosphine-free sub-2 nm particles supported on SBA-15 were obtained.

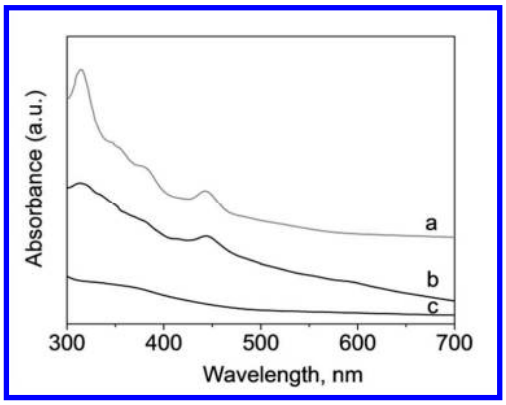

Figure 4. UV-vis spectrum of Au_9 dissolved in CH_2Cl_2 (a) and DR UV-vis spectra of as made $0.1Au_9$/SBA-15 (b) and $0.1Au_9$/SBA_c230 (c).

Although the Au particles were phosphine-free, the kinetics of cyclohexene oxidation in the presence of $0.1Au_9$/SBA_c230 showed an induction period of ca. 3.5 hours. The appearance of catalytic activity correlated with the formation of plasmonic particles (Figure 5), similarly to the behavior observed for SiO_2-based catalysts, discussed earlier. Recycled $0.1Au_9$/SBA_c230

did not show an induction period in cyclohexene oxidation. This result confirmed that phosphine-free Au particles with the sizes below 2 nm are inactive in the cyclohexene oxidation. The change of catalytic behavior of Au particles once they become larger than 2 nm could be due to the transition from non-metallic to metallic properties, which occurs at sizes of ca. 2 nm.[26]

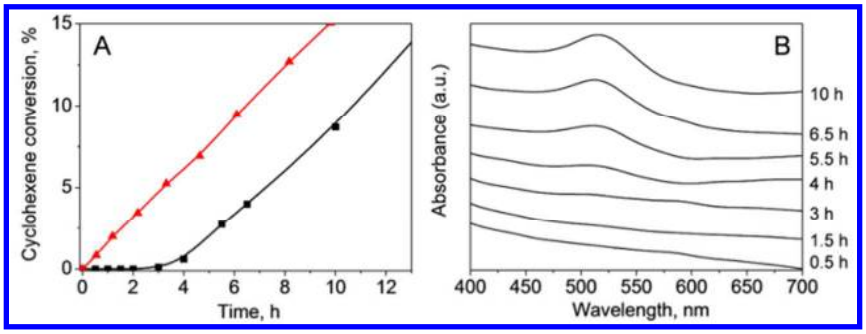

Figure 5. A) Cyclohexene oxidation catalyzed by $0.1Au_9$/SBA_c230 (black) and recycled $0.1Au_9$/SBA_c230 (red). B) DR UV-vis spectra of $0.1Au_9$/SBA_c230 sampled from cyclohexene oxidation at different reaction times.

Numerous examples of catalysis, driven or enhanced by the surface plasmon resonance of Au nanoparticles, have been recently reported.[27-29] Because catalytic activity in our study appeared only when gold nanoparticles larger than 2 nm, i.e. plasmonic particles, were formed, we investigated whether the observed activity was enabled by the SPR. The activity of $0.5Au_9/SiO_2$ in cyclohexene oxidation under ambient light was similar to that in the absence of light, which indicated that catalytic activity was not enhanced by the SPR in this study (Table S2).

XPS spectrum of a post-reaction $0.5Au_9/SiO_2$ showed the $Au4f_{7/2}$ signal centered at 84.0 eV, a binding energy characteristic of bulk neutral gold (Figure 6). No signal at 85.0 eV from pristine Au_9 clusters[30] was detected in the post-reaction catalyst, indicating that most of the gold present in the catalytic system is in the metallic state and no intact clusters are left after the

reaction. Unlike the recently reported activity of positively charged 20-150 nm Au nanoparticles in styrene oxidation,[11] catalytic activity in our case was solely due to the metallic Au^0 particles, as evidenced by the activity of the post-reaction catalysts in the second catalytic cycle.

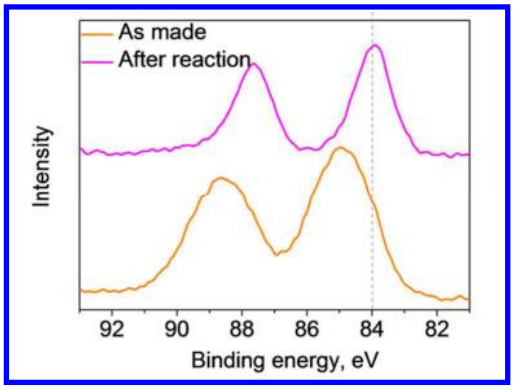

Figure 6. XPS $Au4f_{7/2}$ spectra of as made $0.5Au_9/SiO_2$ and $0.5Au_9/SiO_2$ recovered after 16 h catalytic cycle of cyclohexene oxidation. Dotted vertical line indicates $Au4f_{7/2}$ peak position corresponding to metallic gold.

Finally, colloid stabilizer-free[31] and citrate-stabilized[32] Au nanoparticles were synthesized and deposited onto SiO_2 with the total gold loadings of 0.1 wt%. Four catalysts 0.1Au-9.1/SiO_2, 0.1Au-13.7/SiO_2, 0.1Au-33.9/SiO_2 and 0.1Au-47.4/SiO_2 with particle sizes of 9.1, 13.7, 33.9 and 47.4 nm, respectively, were obtained (Figure S11). All the catalysts were active in cyclohexene oxidation and no induction period was observed (Figure 7). Comparison of initial reaction rates and turnover frequencies (TOFs) of the Au colloid-based catalysts is shown in Table 1. Catalytic activity of 0.1Au/SiO_2 gradually decreased with the increase of Au particle size, which is in accordance with the smaller fraction of surface Au atoms for larger particles. Indeed, TOF values normalized by surface Au are very close for differently sized supported Au nanoparticles (Table 1). This result confirms that Au^0 particles larger than 2 nm are responsible for the observed catalytic activity in the oxidation of cyclohexene.

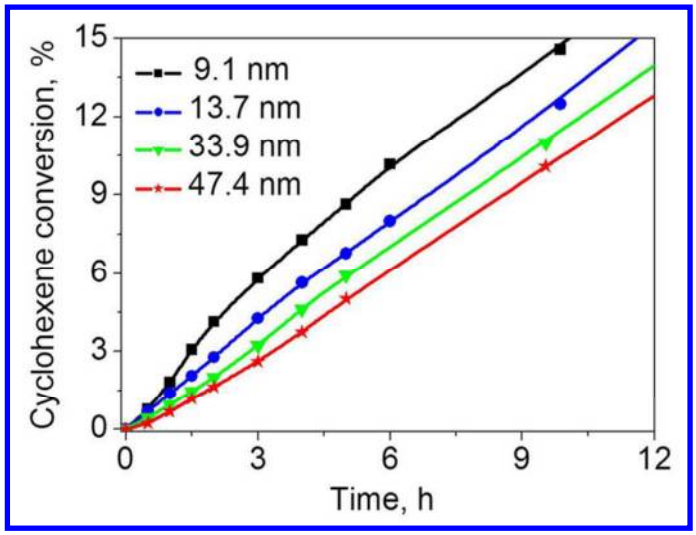

Figure 7. Cyclohexene oxidation catalyzed by 9.1, 13.7, 33.9 and 47.4 nm Au particles supported on SiO_2 with the total gold loading of 0.1 wt%.

Table 1. Comparison of initial reaction rates and TOFs of Au/SiO_2 catalysts in cyclohexene oxidation.

	Catalyst	Reaction rate × 10^6, $mol_{substrate}/s$	TOF_{Au}, s^{-1}	$TOF_{surface\ Au}$, s^{-1}
1	0.1Au-9.1/SiO_2	0.58	1.14	17.5[a]
2	0.1Au-13.7/SiO_2	0.39	0.78	18.0[a]
3	0.1Au-33.9/SiO_2	0.28	0.53	21.7[b]
4	0.1Au-47.4/SiO_2	0.20	0.40	18.9[b]

Fraction of surface Au atoms was estimated assuming [a]spherical and [b]cuboctahedral shape of Au nanoparticles (based on TEM observations).

In this work we showed that only Au^0 particles larger than 2 nm were active in aerobic cyclohexene oxidation; however oxygen adsorption and its dissociative activation on large metallic gold particles were shown to be extremely impeded.[33,34] On the other hand, extended

gold surfaces were long known to catalyze hydrogen abstraction from hydrocarbons,[35] and thus activation of cyclohexene rather than O_2 by gold nanoparticles is the more probable pathway in our case. This suggestion is also supported by the fact that the main product of cyclohexene oxidation in this work is cyclohexenyl hydroperoxide (Figure S12), which is formed in the reaction between dissolved oxygen and cyclohexenyl radicals generated via allylic hydrogen abstraction from cyclohexene. When a sufficient amount of cyclohexenyl hydroperoxide is formed it further acts as a radical chain propagator in cyclohexene autooxidation.[36] A similar mechanism was recently described for cyclohexane oxidation catalyzed by Au/MgO.[37] Higher activity of Au catalysts in cyclohexene oxidation compared to cyclohexane oxidation[12,37,38] can be explained by more facile H-abstraction from an allylic position because allylic C-H is weaker than alkylic C-H bond.

Thus, we showed that at low temperatures sub-2 nm particles are not able to catalyze hydrogen abstraction from the cyclohexene and metallic Au particles larger than 2 nm are the active sites associated with the observed catalytic activity. Such a size effect is opposite to that discovered for oxidation reactions where O_2 activation is involved, e.g. styrene oxidation, for which either sub-2 nm particles[10,34] or large, positively charged particles[11] were suggested as the active sites.

In summary, we established relationship between the size of supported gold nanoparticles and their activity in solvent-free aerobic oxidation of cyclohexene by employing gradually changing catalysts. We showed that phosphine-stabilized gold clusters and phosphine-free Au particles smaller than 2 nm are inactive in this reaction, and that catalytic activity appears only upon formation of sufficient number of metallic particles larger than 2 nm. Further increase in Au particle size results in gradual decrease in catalytic activity, which correlates with the

reduction of the Au surface area. The size-dependency observed in this study is in agreement with the suggested mechanism of substrate activation through the abstraction of hydrogen catalyzed by metallic gold nanoparticles.

EXPERIMENTAL SECTION

Materials

Gold (99.99%), sodium borohydride (>97%), hydrochloric acid (37%, AR grade), nitric acid (65%, AR grade), triphenylphosphine (98%), Pluronic P123 (Mn ~5,800), tetraethyl orthosilicate (98%), cyclohexene (99%, inhibitor-free), 2-cyclohexene-1-ol (95%), 2-cyclohexene-1-one (98%) and cyclohexene oxide (98%) were purchased from Sigma-Aldrich and Merck. Oxygen (99.7%) was obtained from BOC gases. Silicon oxide (Aerosil OX 50) was purchased from Evonik. All materials were used as received.

Catalyst preparation

$Au_9(PPh_3)_8(NO_3)_3$ (Au_9) and $Au_{101}(PPh_3)_{21}Cl_5$ (Au_{101}) were synthesized according to the published procedures.[39,40] As made gold clusters were deposited onto SiO_2 from CH_2Cl_2 solution. A calculated amount of gold cluster dissolved in CH_2Cl_2 (10 mL, 1-2 mg/mL) was added drop-wise to a vigorously stirred suspension of SiO_2 (500 mg) in CH_2Cl_2 (15 mL). The mixture was stirred for 30 min and the solid was collected by centrifugation. Colorless supernatant solution confirmed complete cluster deposition. The catalysts were washed with CH_2Cl_2 (20 mL) and dried under vacuum at room temperature. Deposition of Au_9 cluster onto SBA-15 was performed using the methodology similar to the one described by Liu et al.[41] SBA-15 (500 mg) was suspended in the mixture of C_2H_5OH and CH_2Cl_2 (5 mL, 1:4). Solution of Au_9 cluster (2.3 mg) in the same solvent mixture (5 mL) was slowly added to the suspension of SBA-15 under

vigorous stirring. The mixture was stirred for 2.5 h. The solid was collected via centrifugation, washed with CH_2Cl_2 (10 mL) and dried under vacuum at room temperature.

Stabilizer-free gold nanoparticles were synthesized using method reported by Martin et al.[31] After deposition onto SiO_2 the average diameter of Au particles was 9.1 nm. Citrate-stabilized Au nanoparticles were prepared following a protocol described by Turkevich et al.[32] Briefly, 450 mL of 0.24 mM $HAuCl_4$ and 1.6 mM sodium citrate solution was heated at 70 ˚C for 1 hour. The resulting red solution containing 13.9 nm Au particles was cooled down using ice bath. 33.9 nm particles were prepared by heating 50 mL of 0.3 mM $HAuCl_4$ and 0.58 mM sodium citrate solution at 90 ˚C for 5 minutes. 47.4 nm particles were prepared by heating 50 mL 1.2 mM $HAuCl_4$ and 1.9 mM sodium citrate at 60 ˚C for 2 hours. The resulting colloid Au particles were deposited on SiO_2 from aqueous solutions. A calculated volume of fresh Au nanoparticles solution in water was added to SiO_2 (0.5 g). Mixture was sonicated for 1 minute and water was slowly removed from the suspension using rotary evaporator. The resulting solid was collected, dried under vacuum at room temperature and characterized using TEM.

Catalyst characterization

Catalysts were characterized using transition electron microscopy (TEM), X-ray photoelectron spectroscopy (XPS), diffuse-reflectance UV-vis (DR UV-vis). Gold loadings were established using atomic absorption spectroscopy (AAS) on a VARIAN SpectrAA 220FS. TEM analysis was performed using Philips CM200 operating at 200 kV. Samples for TEM analysis were suspended in diethyl ether and deposited on holey-carbon coated Cu grids. At least 100 particles were measured to plot size distributions. DR UV-vis spectra were recorded using Cintra 404 (GBC Scientific Equipment) spectrometer. XPS was conducted on a Kratos Axis DLD

spectrometer with a monochromated Al-Kα X-ray source. The samples were pressed into indium as the mounting medium. A supply of low energy electrons was used for charge neutralization. Survey spectra were recorded with a pass energy of 80 eV and high-resolution spectra with a pass energy of 40 eV. Binding energies were normalized with respect to the position of the adventitious C1s peak at 285.0 eV.

Catalytic experiments

Catalytic activity of Au catalysts was tested in aerobic solvent-free cyclohexene oxidation without addition of radical initiator. Kinetic studies of cyclohexene oxidation were performed in a glass reactor equipped with a reflux condenser. 10 mL of cyclohexene containing 0.2 M of n-decane as an internal standard, 100 mg of catalyst and Teflon-coated magnetic stirrer were loaded into 100 mL 2-necked glass round bottom flask. System was flushed with O_2 three times and connected to a rubber balloon filled with O_2. The mixture was magnetically stirred at 65 °C. Samples of reaction mixture were taken using glass syringe. Reaction was stopped by cooling the reactor to room temperature; condenser was rinsed with 5 mL of diethyl ether and the reaction mixture was separated from the solid catalyst by centrifugation. Catalysts were washed with diethyl ether and dried under vacuum at room temperature before recycling. Each experiment was reproduced at least three times. The typical standard errors of independent catalytic tests were below 1.5 %. Turnover frequencies were calculated from the initial rates of cyclohexene oxidation.

The liquid samples were analyzed by gas chromatography (GC-FID) using Shimadzu GC-2010 equipped with an Rxi-5SilMS capillary column (30 m × 0.25 mm × 0.25 μm). The products of cyclohexene oxidation were identified by GC-MS (Shimadzu GCMS-QP2010) and

quantified using solutions of reference compounds with known concentrations. The concentration of cyclohexenyl hydroperoxide was established using iodometric titration.[42] Addition of PPh_3 to the reaction mixture prior to GC analysis did not change the concentration of 2-cyclohexene-1-one, determined from GC analysis, which implies that there was no cyclohexenyl hydroperoxide decomposition during GC analysis.[43] Concentration of cyclohexenyl hydroperoxide was calibrated by comparison of GC data and iodometric titration results and was further calculated directly from GC results.

ASSOCIATED CONTENT

Supporting Information.

Cluster and catalyst characterization details, additional catalytic data. This material is available free of charge via the Internet at http://pubs.acs.org.

AUTHOR INFORMATION

Corresponding Author

*E-mail: vladimir.golovko@canterbury.ac.nz

Author Contributions

‡These authors contributed equally

Notes

The authors declare no competing financial interests.

ACKNOWLEDGMENT

We would like to thank Dr Colin Doyle from RCSMS for XPS analysis; Campbell McNicoll and Dr Tim Kemmitt from Callaghan Innovation NZ for their help with surface area measurements. We thank Prof Bryce Williamson for valuable discussions. This work was supported by the University of Canterbury and the MacDiarmid Institute. B.D. thanks the MacDiarmid Institute for the research scholarship and D.O. thanks the University of Canterbury for UC Doctoral scholarship.

REFERENCES

(1) Haruta, M.; Kobayashi, T.; Sano, H.; Yamada, N. *Chem. Lett.* **1987**, 405.
(2) Hutchings, G. J. *J. Catal.* **1985**, *96*, 292.
(3) Corma, A.; Garcia, H. *Chem. Soc. Rev.* **2008**, *37*, 2096.
(4) Stratakis, M.; Garcia, H. *Chem. Rev. (Washington, DC, U. S.)* **2012**, *112*, 4469.
(5) Della, P. C.; Falletta, E.; Rossi, M. *Chem. Soc. Rev.* **2012**, *41*, 350.
(6) Haruta, M. *Catal. Today* **1997**, *36*, 153.
(7) Haruta, M. *J. New Mater. Electrochem. Syst.* **2004**, *7*, 163.
(8) Hvolbæk, B.; Janssens, T. V. W.; Clausen, B. S.; Falsig, H.; Christensen, C. H.; Nørskov, J. K. *Nano Today* **2007**, *2*, 14.
(9) Schubert, M. M.; Hackenberg, S.; van Veen, A. C.; Muhler, M.; Plzak, V.; Behm, R. J. *J. Catal.* **2001**, *197*, 113.
(10) Turner, M.; Golovko, V. B.; Vaughan, O. P. H.; Abdulkin, P.; Berenguer-Murcia, A.; Tikhov, M. S.; Johnson, B. F. G.; Lambert, R. M. *Nature (London, U. K.)* **2008**, *454*, 981.
(11) Wang, L.; Zhang, B.; Zhang, W.; Zhang, J.; Gao, X.; Meng, X.; Su, D. S.; Xiao, F.-S. *Chem. Commun. (Cambridge, U. K.)* **2013**, *49*, 3449.
(12) Liu, Y.; Tsunoyama, H.; Akita, T.; Xie, S.; Tsukuda, T. *ACS Catal.* **2011**, *1*, 2.
(13) Xu, L.-X.; He, C.-H.; Zhu, M.-Q.; Wu, K.-J.; Lai, Y.-L. *Catal. Lett.* **2007**, *118*, 248.
(14) Haider, P.; Kimmerle, B.; Krumeich, F.; Kleist, W.; Grunwaldt, J.-D.; Baiker, A. *Catal. Lett.* **2008**, *125*, 169.
(15) Haider, P.; Urakawa, A.; Schmidt, E.; Baiker, A. *J. Mol. Catal. A: Chem.* **2009**, *305*, 161.
(16) Liu, Y.; Tsunoyama, H.; Akita, T.; Tsukuda, T. *Chem. Lett.* **2010**, *39*, 159.
(17) Sun, K.-Q.; Luo, S.-W.; Xu, N.; Xu, B.-Q. *Catal. Lett.* **2008**, *124*, 238.
(18) Tana; Wang, F.; Li, H.; Shen, W. *Catal. Today* **2011**, *175*, 541.
(19) Kamat, P. V. *J. Phys. Chem. B* **2002**, *106*, 7729.
(20) Kelly, K. L.; Coronado, E.; Zhao, L. L.; Schatz, G. C. *J. Phys. Chem. B* **2003**, *107*, 668.
(21) Henglein, A. *Langmuir* **1999**, *15*, 6738.
(22) Kilmartin, J.; Sarip, R.; Grau-Crespo, R.; Di, T. D.; Hogarth, G.; Prestipino, C.; Sankar, G. *ACS Catal.* **2012**, *2*, 957.
(23) Woehrle, G. H.; Hutchison, J. E. *Inorg. Chem.* **2005**, *44*, 6149.

(24) Zhao, D.; Feng, J.; Huo, Q.; Melosh, N.; Frederickson, G. H.; Chmelka, B. F.; Stucky, G. D. *Science (Washington, D. C.)* **1998**, *279*, 548.
(25) Liu, Y.; Tsunoyama, H.; Akita, T.; Tsukuda, T. *J. Phys. Chem. C* **2009**, *113*, 13457.
(26) Bond, G. C.; Thompson, D. T. *Catal. Rev.* **1999**, *41*, 319.
(27) Vankayala, R.; Sagadevan, A.; Vijayaraghavan, P.; Kuo, C.-L.; Hwang, K. C. *Angew. Chem., Int. Ed.* **2011**, *50*, 10640.
(28) Sun, M.; Xu, H. *Small* **2012**, *8*, 2777.
(29) Christopher, P.; Xin, H.; Linic, S. *Nat. Chem.* **2011**, *3*, 467.
(30) Battistoni, C.; Mattogno, G.; Cariati, F.; Naldini, L.; Sgamellotti, A. *Inorg. Chim. Acta* **1977**, *24*, 207.
(31) Martin, M. N.; Basham, J. I.; Chando, P.; Eah, S.-K. *Langmuir* **2010**, *26*, 7410.
(32) Turkevich, J.; Stevenson, P. C.; Hillier, J. *Discuss. Faraday Soc.* **1951**, *No. 11*, 55.
(33) Janssens, T. V. W.; Clausen, B. S.; Hvolbaek, B.; Falsig, H.; Christensen, C. H.; Bligaard, T.; Norskov, J. K. *Top. Catal.* **2007**, *44*, 15.
(34) Alves, L.; Ballesteros, B.; Boronat, M.; Cabrero-Antonino, J. R.; Concepción, P.; Corma, A.; Correa-Duarte, M. A.; Mendoza, E. *J. Am. Chem. Soc.* **2011**, *133*, 10251.
(35) Bond, G. C. *Gold Bull.* **1972**, *5*, 11.
(36) Mahajani, S. M.; Sharma, M. M.; Sridhar, T. *Chem. Eng. Sci.* **1999**, *54*, 3967.
(37) Conte, M.; Liu, X.; Murphy, D. M.; Whiston, K.; Hutchings, G. J. *Phys. Chem. Chem. Phys.* **2012**, *14*, 16279.
(38) Lue, G.; Ji, D.; Qian, G.; Qi, Y.; Wang, X.; Suo, J. *Appl. Catal., A* **2005**, *280*, 175.
(39) Weare, W. W.; Reed, S. M.; Warner, M. G.; Hutchison, J. E. *J. Am. Chem. Soc.* **2000**, *122*, 12890.
(40) Wen, F.; Englert, U.; Gutrath, B.; Simon, U. *Eur. J. Inorg. Chem.* **2008**, *2008*, 106.
(41) Liu, Y.; Tsunoyama, H.; Akita, T.; Tsukuda, T. *J. Phys. Chem. C* **2009**, *113*, 13457.
(42) Mair, R. D.; Graupner, A. J. *Anal. Chem. (Washington, DC, U. S.)* **1964**, *36*, 194.
(43) Shul'pin, G. B. *J. Mol. Catal. A: Chem.* **2002**, *189*, 39.

SYNOPSIS